Supplement

Neoadjuvant immune checkpoint blockade before chemoradiation for cervical squamous carcinoma (GINECO window-of-opportunity COLIBRI study): a phase II trial

Isabelle Ray-Coquard et al.

Supplementary Methods

Briefly, 4 µm-thick formalin-fixed paraffin-embedded sample sections were stained in a cyclic manner using OPAL technology (Akoya Biosciences, MA, USA) and the Leica Bond RX (Leica Biosystems, Nussloch, Germany) with an antibody panel described in Supplementary Table 3. DAPI was used for nuclei detection and slides were digitalized with a multispectral scanner (PhenoImager HT, Akoya Biosciences). After denoising of digital images, the whole evaluable tumor area was annotated by a pathologist after reviewing a hematoxylin-eosin (HE)-stained section. Quantitative analysis was performed by machine learning using the inForm automated image analysis software (version 2.5, Akoya Biosciences), allowing phenotyping of the different cell types in the stroma versus tumor areas segmented based on pan-CK staining (Supplementary Fig. 5). Densities of each cell phenotype were quantified and expressed as number of cells per mm^2. All data were consolidated using R studio (PhenoptrReports, Akoya Biosciences). Results reported in this paper relate to the total area (tumor plus stroma).

Supplementary Table 1 | Summary of chemoradiation delivery

Chemoradiation	Patients (n = 40)
Carboplatin, No. (%)[a]	3 (8)
Cisplatin, No. (%)	39 (98)
Chemotherapy treatment modification, No. (%)	6 (15)[b]
Radiotherapy dose modification, No. (%)	0
Lymph node boost, No. (%)	27 (68)
Median (range) chemoradiation duration, months	1.2 (1.1–2.3)
Brachytherapy, No. (%)	36 (90)[c]

[a]Among the three patients who received carboplatin, one received one cycle of carboplatin (week 3) and cisplatin for all other cycles, one received cisplatin for weeks 1, 2 and 3 and switched to carboplatin for weeks 4, 5, and 6, and one received carboplatin for weeks 1, 2 and 3 and no cisplatin.
[b]Chemotherapy was temporarily discontinued because of adverse events in five patients.
[c]Among the four patients who did not receive brachytherapy, three had external tumor boost with external beam radiotherapy and one decided not to have brachytherapy.

Supplementary Table 2 | Most common (≥10% of patients) adverse events by treatment phase

AE, No. (%)	Neoadjuvant ipilimumab/nivolumab (n = 40)	Chemoradiation (n = 40)	Maintenance nivolumab (n = 39)
Anemia	5 (13)	19 (48)	3 (8)
Grade 3	0	2 (5)	0
Thrombocytopenia	0	7 (18)	1 (3)
Grade 4	0	1 (3)	0
Lymphopenia	1 (3)	7 (18)	5 (13)
Grade 3	0	4 (10)	2 (5)
Leukopenia	0	6 (15)	2 (5)
Grade 3	0	0	1 (3)
Neutropenia	0	4 (10)	1 (3)
Diarrhea	6 (15)	23 (58)	7 (18)
Grade 3	0	4 (10)	0
Constipation	5 (13)	7 (18)	3 (8)
Nausea	2 (5)	21 (53)	1 (3)
Grade 3	0	1 (3)	0
Vomiting	0	5 (13)	1 (3)
Grade 3	0	1 (3)	0
Abdominal pain	2 (5)	5 (13)	3 (8)
Asthenia	11 (28)	15 (38)	10 (26)
Grade 3	1 (3)	1 (3)	1 (3)
Fatigue	1 (3)	4 (10)	2 (5)
Decreased appetite	4 (10)	4 (10)	2 (5)
Weight decreased	0	5 (13)	0
Hypothyroidism	0	9 (23)	5 (13)
Pruritus	8 (20)	0	2 (5)
Pollakiuria	0	5 (13)	2 (5)
Metrorrhagia	6 (15)	2 (5)	2 (5)

Supplementary Table 3 | Antibodies for 7-color mIF staining

Antibody	Description	Reference	Dilution	Staining localization
Ki67	Proliferation marker	M7240 DAKO	1/200	Nuclear
CD3	T lymphocytes	A0452 DAKO	1/100	Membrane
CD8	$CD8^+$ T lymphocytes	M7103 DAKO	1/50	Membrane
CD20	B lymphocytes	M0755 DAKO	1/600	Membrane
Pan-CK	Tumor cell marker	M3515 DAKO	1/92	Cytoplasmic
FOXP3	Regulatory T cells	PA0263 Leica	Ready to use	Nuclear

Supplementary Fig. 1 | Summary of sample availability (the main reason for missing samples was technical sample failure). a Patient flow by timepoint and analysis type. **b** Availability of paired samples for mIF and/or HTG analysis. BL, baseline; HTG, high-throughput genomic; mIF, multiplex-immunofluorescence; RTCT, chemoradiation.

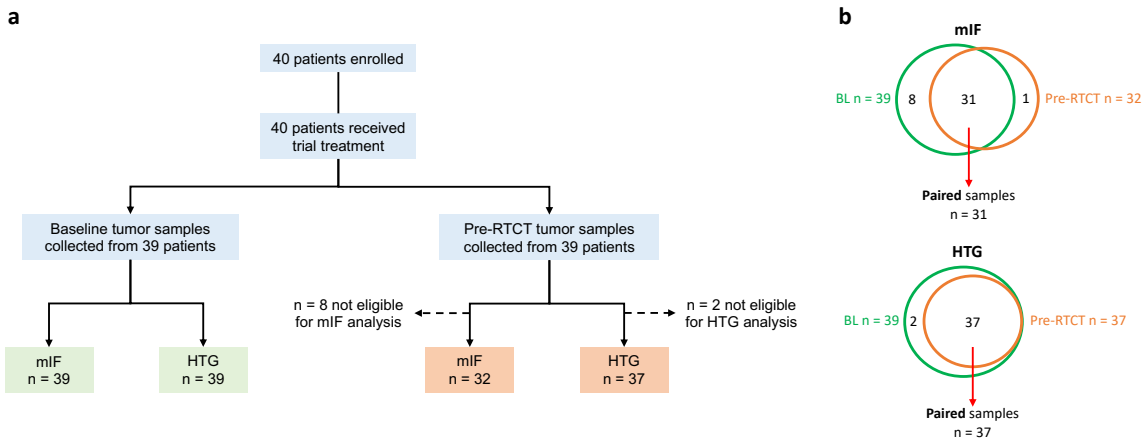

Supplementary Fig. 2 | Association of immune parameters with therapeutic response to trial treatment. a Heatmap showing immune parameters in baseline samples (before immunotherapy) according to response evaluated at EOT; CR (n = 31) and non-CR (n = 9). **b** Heatmap showing immune parameters in samples before chemoradiation according to response before chemoradiation; non-PR (n = 35) and PR (n = 5). Each column represents a patient and each row an immune parameter; cell color denotes the Z-score. Within each response group, patients were sorted left to right by decreasing $CD8^+$ Teff density. Group differences for each immune parameter (a: non-CR vs CR; b: non-PR vs PR) were assessed using the two-sided Mann–Whitney U test and non-adjusted *P*-values are shown. **c** Graphs depicting the association between selected immune parameters quantified by mIF from samples collected at BL (upper graphs) or before RTCT (lower graphs) and response to treatment. Patients were stratified by clinical response before RTCT (non-PR vs PR, left graphs) or at EOT (non-CR vs CR, right graphs). Each dot represents a patient measured once at the indicated timepoint (biological replicates only; no technical replicates). Statistical differences between groups were tested using the two-sided Mann–Whitney U test with no adjustment for multiple comparisons. No separate control group was used as comparisons were performed between response-defined groups within the same cohort. Source data are provided as a Source Data file. BEF, before chemoradiation; BL, baseline; CR, complete response; EOT, end of treatment; HTG, high-throughput genomic; PD, disease progression; PR, partial response; RTCT, chemoradiation; SD, stable disease; Teff, effector T cells; Treg, regulatory T cells.

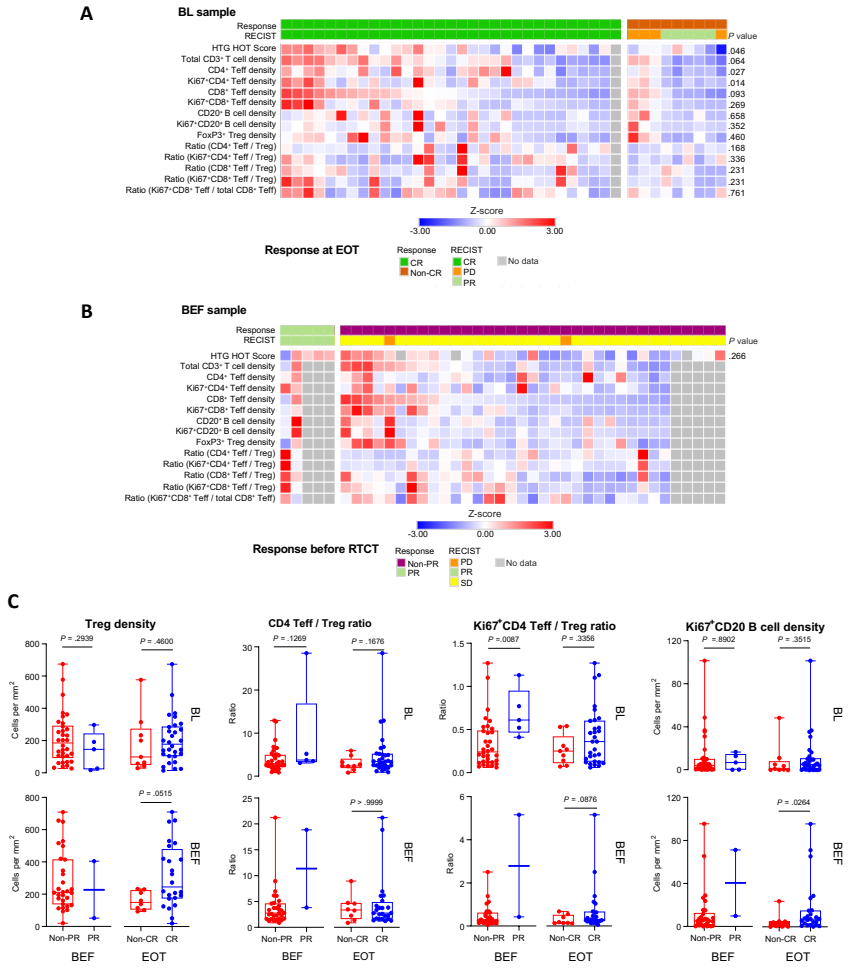

Supplementary Fig. 3 | Quantification of TLS by mIF. a Workflow used to quantify TLS from mIF whole-slide images using the CD3, CD20, and Ki67 markers. Manual annotations were made to quantify lymphoid T/B aggregates, immature TLS (with Ki67$^-$ B cell follicles), and mature TLS (with Ki67$^+$ B cell follicles). **b** Pie charts showing the relative proportions of these three categories in BL versus BEF samples. **c** Sankey diagram showing the evolution of TLS status on ICB for the 31 patients with paired BL vs BEF samples. BEF, before chemoradiation; BL, baseline; ICB, immune checkpoint blockade; mIF, multiplex immunofluorescence; TLS, tertiary lymphoid structures.

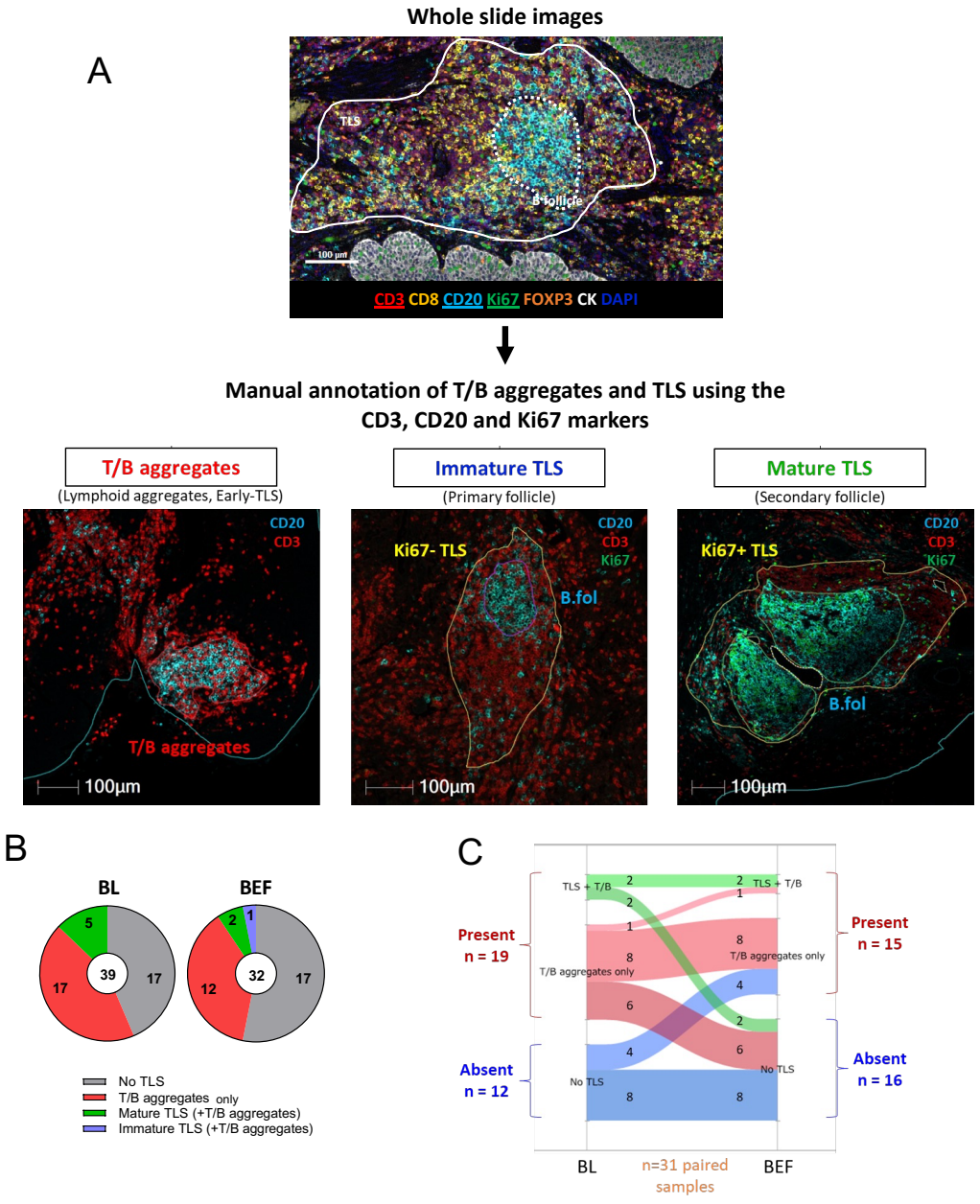

Supplementary Fig. 4 | Association between pre-treatment immune parameters and irAEs. Patients were stratified according to clinically diagnosed irAEs (CTCAE v5.0) into no irAE/G1 (n = 18) and G2/G3 (n = 21) groups. **a** Graph depicting the *P*-values of selected tumor immune parameters between the two groups at baseline (Mann-Whitney U tests). **b** Boxplots of selected immune cell parameters. Source data are provided as a Source Data file. CTCAE, Common Terminology Criteria for Adverse Events; G, grade; irAE, immune-related adverse event; Teff, T effector cells; Treg, regulatory T cells.

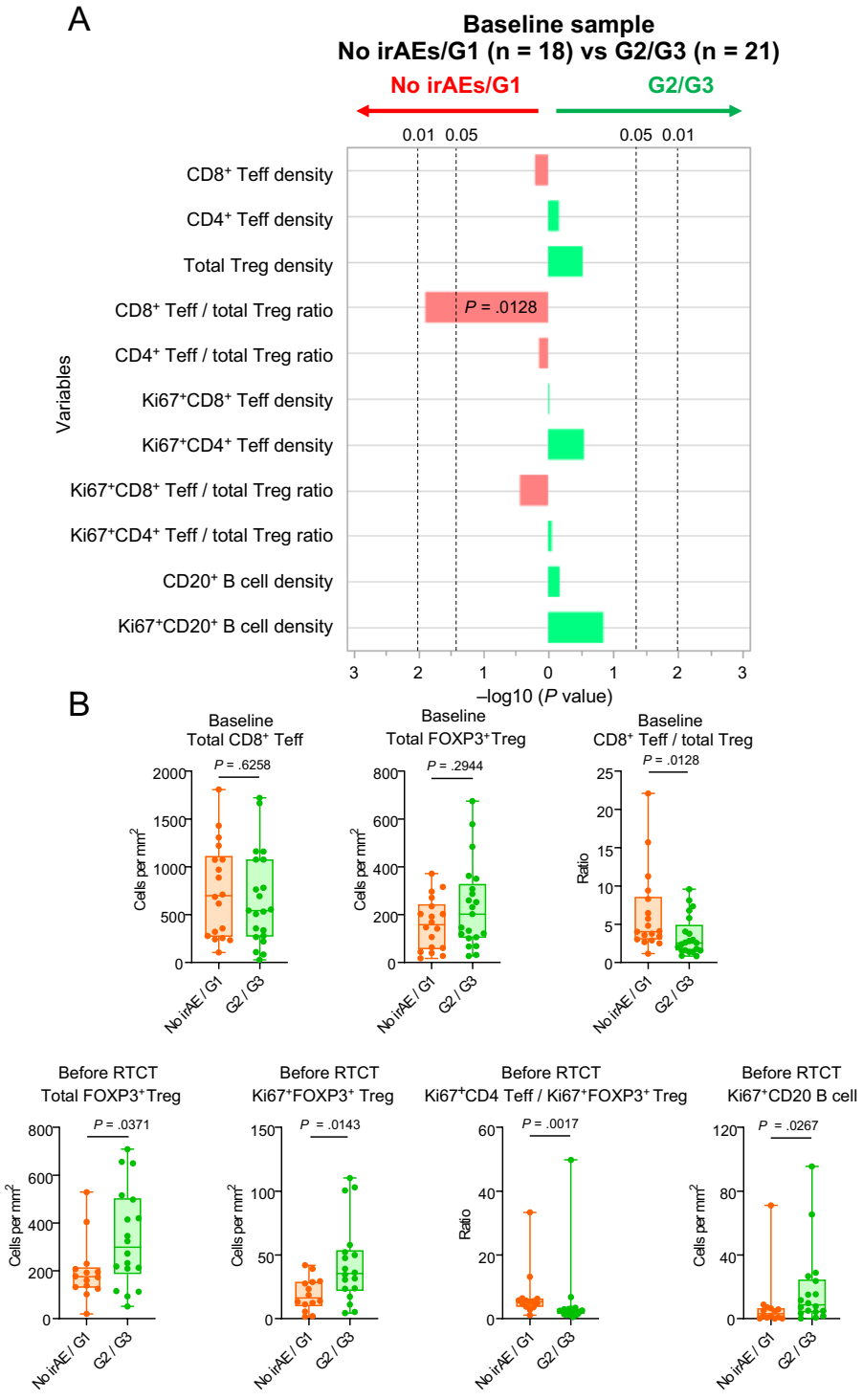

Supplementary Fig. 5 | Analytical pipeline used for quantitative analysis of 7-color mIF digital images by machine learning. a Annotation of ROI. Whole-slide images were divided into tiles/ROI (4,671 in total for the cohort) and representative ROIs (77) were selected using the Phenochart viewer (Akoya) to train and validate algorithms. **b** mIF analytical pipeline. After composite image unmixing, a tissue segmentation algorithm was designed using DAPI and CK staining to distinguish tumor, stromal, and artefacts areas, and cell segmentation was performed using the DAPI and Ki67 channels. The cell phenotyping algorithm was trained with visual inspection of every marker. Based on theoretical marker co-expression patterns, 4 cell phenotyping algorithms were developed, CD3-CD20-CK, CD8, Ki67 and FOXP3, and validated. **c** Representative native images (top) images with cell phenotype mapping (bottom). IF, immunofluorescence; mIF, multiplex-immunofluorescence; ROI, regions of interest.